I&EC research
Industrial & Engineering Chemistry Research

Article

pubs.acs.org/IECR

Char Structure and Combustion Kinetics of a Phenolic-Impregnated Honeycomb Material

Carmen Branca*[,†] and Colomba Di Blasi[‡,§]

[†]Istituto di Ricerche sulla Combustione, CNR, Piazzale V. Tecchio, 80125 Napoli, Italy

[‡]Dipartimento di Ingegneria Chimica, dei Materiali e della Produzione Industriale, Università degli Studi di Napoli "Federico II", Piazzale V. Tecchio, 80125 Napoli, Italy

[§]Distretto Tecnologico sull'Ingegneria dei Materiali Polimerici e Compositi e Strutture (IMAST) Piazza Bovio 22, 80133 Napoli, Italy

ABSTRACT: The combustion behavior of a honeycomb material used for the core in sandwich panels, consisting of aramid fiber sheets (Nomex) dipped in a phenolic resin, is studied. Char, produced from pyrolysis of thick samples at 950 K, preserves the honeycomb structure, but the total volume is highly reduced in spite of an increase in the wall thickness. Following softening, the more internal fibers lose their shape, giving rise to a highly porous swelled char. Instead, the more external ones, trapped by the resin char, still show their original shape but with evident shrinkage. Thermogravimetric curves in air are used to formulate a combustion mechanism. It consists of three reactions for the stage of oxidative decomposition of the honeycomb material and one reaction for combustion of the resulting char. Activation energies for the various steps vary in a narrow range of high values (190−256 kJ/mol), testifying low reactivity.

1. INTRODUCTION

One of the main aims of material research is to develop lighter, cheaper, and mechanical-resistant structures. Fiber-reinforced composites present high weight-specific stiffness and strength properties and are extensively applied in various industrial sectors, especially maritime, railway, and aeronautical transportation industries.[1] An even better behavior in relation to the above properties may be achieved by sandwich panels, which are multilayered structures consisting of high-strength stiff skins bonded to a more flexible and light core.[2,3] These lightweight structures are mainly used for interior panels of transportation applications and sporting goods and, to a minor extent, in civil infrastructures such as highway bridges and building constructions. Skins are typically made of metal, resin-based glass-fiber-reinforced plastics or carbon-fiber-reinforced plastics. The core material is frequently made of flexible foams, honeycomb materials, or balsa wood. Despite the excellent mechanical properties of sandwich panels, the constituent polymeric materials are intrinsically flammable, so their fire response should be adequately taken into account in practical applications.

A particularly widespread core material consists of a phenolic resin-impregnated aramid paper honeycomb structure commonly known as Nomex.[4] The flammability properties of fire-retarded fabrics, based on aramid fibers, have recently raised some interest[5−7] because they represent profitable niche markets, for industrial and military uses, in the global textile complex. Also, exploitation of polyaramid fibers as precursors of activated carbon fibers has motivated studies on their pyrolysis behavior,[8−11] also including a detailed analysis of gas composition.[12] However, the flammability characteristics of honeycomb composite materials are reported[13] to be significantly affected by the presence of phenol−formaldehyde resin. On the other hand, fundamental studies on the decomposition characteristics and oxidation kinetics of these composite materials are not available. In particular, the search of kinetic mechanisms is of paramount importance for the development of predictive transport models,[14] which can be applied to understand and improve the action of advanced fire retardants[15−18] or the fire behavior of multilayered structures.[19,20] Predictive models aim at a detailed description of each process in the governing equations for the thermal response of a composite material/structure without the use of adjustable parameters. Indeed, peculiar of this approach is the use of intrinsic chemical kinetics and physical properties of the composites, previously evaluated from carefully conducted experiments that are different from those used for the experimental validation of the entire model. In general, these models are useful for interpreting the results of standard tests for material qualification and for developing a multidisciplinary design of innovative appliances, thus reducing the experimental efforts and related costs. The understanding of the fundamentals of material degradation can also contribute to the design of composites with improved performances under fire conditions and the development of new flame retardants.

This study examines the changes undergone by a commercial honeycomb material, constituted by aramid fibers coated with a phenolic resin, when subjected to high-temperature pyrolysis. Also, thermogravimetric measurements are made in air of this material and are used to formulate a multistep combustion mechanism including evaluation of the related kinetic parameters, as a first step toward the development of comprehensive predictive models for the fire behavior of sandwich structures.

Received: July 30, 2013
Revised: September 13, 2013
Accepted: September 19, 2013
Published: September 19, 2013

dx.doi.org/10.1021/ie402470z | *Ind. Eng. Chem. Res.* 2013, 52, 14574−14582

2. MATERIALS AND METHODS

2.1. Materials. The material examined is produced by Hexcel with the commercial name of HexWeb HRH-10.[21] It is manufactured from aramid fiber sheets (Nomex). A thermosetting adhesive is used to bond these sheets at the nodes, and after expansion to a hexagonal configuration, the block is dipped in phenolic resin. After curing of the resin, slices are cut to the desired thickness. Specifically, HexWeb HRH-10 is extensively used in the aerospace industry and several commercial areas as a core material in sandwich panels (interior panels of commercial aircrafts, exterior aircraft parts, surfboards, and high-performance boats).

2.2. Experimental Details. To investigate the thermogravimetric behavior of the honeycomb material in air, a system previously developed and extensively applied to investigate solid conversion under conditions of kinetic control[22−28] is used. The oxidation of the composite solid is made to occur under known thermal conditions with proper control of the sample temperature (measured by a close-coupled thin thermocouple), using the intensity of the applied radiative heat flux as the adjustable variable. In this way, possible temperature overshoots, associated with the combustion exothermicity, which would lead to erroneous kinetic analysis, are avoided.[29,30] The characteristic size of the process is the thickness of the sample layer, whose limit value for kinetic control depends on the nature of the solid fuel and the heating conditions.

Milling to produce powdered samples, as is generally used in thermogravimetric analysis, has proven to be difficult for the composite material under study. Thus, the walls of the honeycomb cell (aramid fiber sheet coated with phenolic resin) are used for this purpose, more precisely 2 mm × 20 mm strips, with a weight of 3.6 mg (predrying is made by exposure of the sample in an oven at 373 K overnight). In this way, the sample thickness is that of the cell wall. Although this appears to be around 100 μm and thus approximately coincident with those previously employed during the kinetically controlled combustion of both organic and synthetic polymers,[23−25,27−29,31] large deviations of the sample temperature with respect to the programmed value (for values above 750 K) are already observed for a heating rate of 10 K/min. In general, to avoid significant deviations, the response of the PID control system should be faster than the combustion rate. Because this is determined by the sample heating rate/temperature and solid reactivity, for the material under study, it is necessary to carry out the experiments at heating rates below 10 K/min. More precisely, values of 3, 5 and 7 K/min are used, which result in excellent temperature control. Moreover, the final temperature is set at 950 K because this value is sufficiently high for the sample to attain complete conversion. Each thermogravimetric measurement is made in triplicate, showing good repeatability (maximum deviations between the measured weight loss curves are always in the range of 0.1−0.3%).

Pyrolysis, using nitrogen as an inert gas, of predried thick samples, in the shape of parallelepiped, with length 21 mm and width 15 mm × 16 mm, is also performed to investigate the morphological changes undergone by the char residue. The sample is suspended within less than 3 s by means of a stainless steel mesh basket, in the isothermal zone of a cylindrical stainless steel reactor,[23,31,32] previously preheated at a temperature of 950 K. Each test is again made in triplicate, showing excellent reproducibility in relation to the char yield. The temperature is recorded by a thermocouple, in close contact with the cell wall, at the median section of the sample. The structure of the charred residue, collected at the conclusion of the tests, is studied by means of scanning electron microscopy (SEM) images. Also, the char produced from the parallelepiped sample is milled with particle sizes below 80 μm and subjected to thermogravimetric analysis in air (3.5 mg distributed over a surface of the same size as that of the strips used for the thermogravimetric measurements of the composite material) for a heating rate of 5 K/min up to a final temperature of 950 K. Smaller particle sizes and sample mass do not give rise to any variations in the measured mass loss rates, indicating that conversion takes place under kinetic control.

3. RESULTS

In the first part of this section, the structure of the char produced from pyrolysis of the honeycomb material is discussed. Then the main characteristics shown by the thermogravimetric curves are presented and used to formulate a multistep oxidation mechanism. Finally, the related kinetic constants are estimated.

3.1. Morphological Structure of Char. Pyrolysis of the thick sample of the honeycomb material, at 950 K, is observed to take place in about 15 min, when the resulting charred residue attains a constant weight, corresponding to 56% of the initial value. The sample center reaches the final temperature in about 80 s, but the maximum heating rate, about 12 K/s, is attained for times shorter than 40 s. At a first glance, it appears that the material retains its honeycomb structure after pyrolysis, but shrinkage occurs at a certain extent, as shown in Figure 1. The

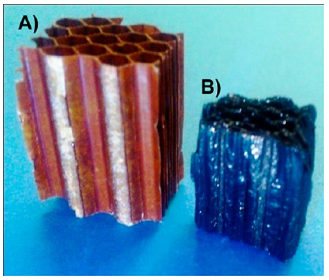

Figure 1. Snapshot of the thick honeycomb sample before (A) and after (B) pyrolysis at 950 K.

length (direction parallel to the fibers) is reduced by about 15%, while one side of the cross section (the glued one with an original size of 16 mm) is reduced by about 50% and the other remains unvaried, leading to a reduction in the total volume of about 43%. However, it is important to notice that the original structure of the sample does not collapse, following pyrolysis.

Important morphological changes occur at the microscopic level, as observed by means of SEM images (Figure 2A−F), which compare the structure of the original, unreacted cell and the corresponding charred one (sample cross section). The char cell still shows a hexagonal structure, but its shape becomes irregular and narrower (Figure 2A,B). Indeed the two diagonals of the hexagon shorten from 4.3 and 3 mm to 3.4 and 1.8 mm, respectively (reductions in the enclosed area of about 65%). Instead, the thickness of the cellular structure is significantly augmented, as can be observed from the images reported in Figure 2C−F. The aramid fibers of the virgin material are intertwined with a high degree of interaction. Moreover, the external surface is smooth because of a phenolic resin coating. Upon pyrolysis, the structure puts into evidence a central junction line, corresponding to the bonding of the aramid fiber

dx.doi.org/10.1021/ie402470z | Ind. Eng. Chem. Res. 2013, 52, 14574−14582

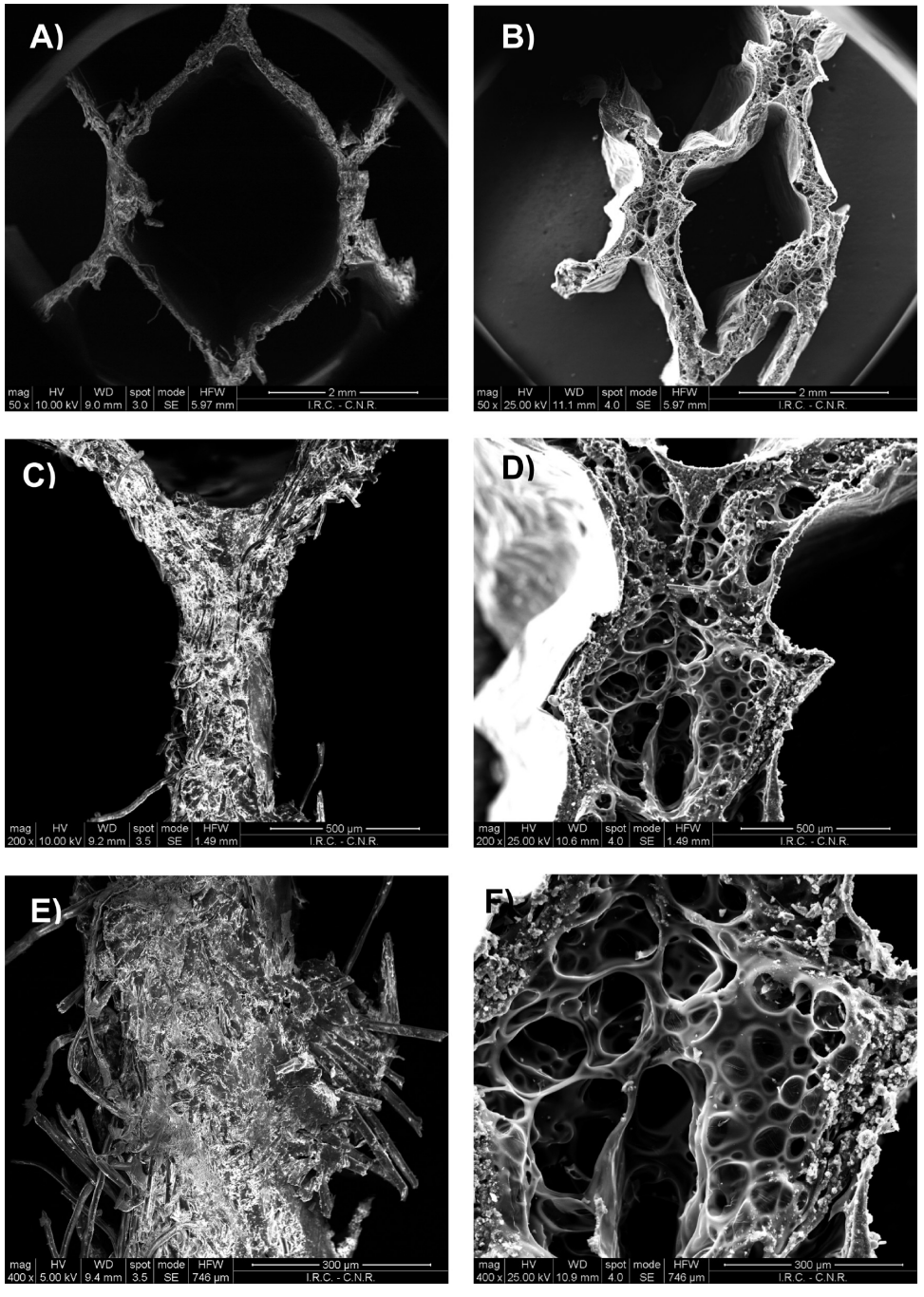

Figure 2. SEM images of the hexagonal sample cell (cross section) before (A, C, and E) and after (B, D, and F) pyrolysis at 950 K of the composite material.

sheets, surrounded by a highly porous matrix, most likely representing the residue generated from Nomex decomposition, and a more external layer characterized by a more dense structure, presumably mainly generated from decomposition of the phenolic resin. According to the producers,[21] Nomex softens between 503 and 533 K, and the release of volatile products at higher temperatures causes the nucleation of bubbles, which burst, giving rise to the formation of pores of different sizes. The formation of bubbles also causes the swelling of the cell walls, whose thickness increases from about 300 μm (virgin material) to about 500−600 μm (char). A further increase in the temperature then results in cross-linking and solidification of the molten phase. Parts D and F of Figure 2 also reveal that pores present a decreasing size as the external surfaces are approached. This can be attributed to the attainment of higher gas pressure across the more internal zone, as is generally observed during pyrolysis of porous solids.[20,33] Moreover, the structure of the skin-deep layer is essentially determined by the thermal behavior of the phenolic resin because the high-molecular-weight aromatic material, remaining after the scission reactions, condenses to form high yields of char.[1,34]

Parts A−D of Figure 3 compare the surface features of the cell wall for the virgin material and char. Parts A and C of Figure 3, which refer to the wall without resin coating, show the original structure of the aramid sheet, with pairs of fibers that stretch along various directions. More interesting is the structure shown

dx.doi.org/10.1021/ie402470z | *Ind. Eng. Chem. Res.* 2013, 52, 14574−14582

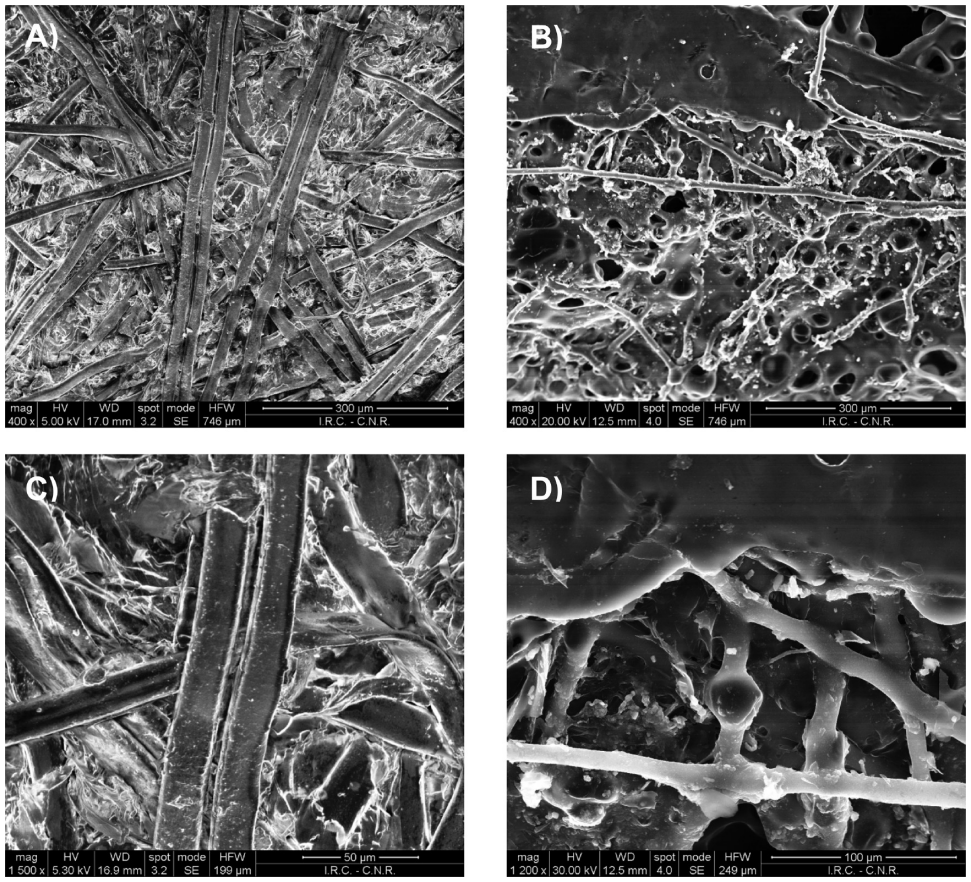

Figure 3. SEM images of the cell walls (surface) before (A and C) and after (B and D) pyrolysis at 950 K of the composite material.

by the charred residue through Figure 3B,D. The upper part refers to a zone almost completely coated by the char generated from the resin. The lower part, corresponding to a zone where the two sheets have been torn before pyrolysis, still shows a few original fibers, embedded in a fuselike material. It can be reasonably guessed that char, formed from decomposition of the phenolic resin and/or thermosetting adhesive, contributes to preserve the original shape of a few fibers, despite their softening (a bubble is clearly visible on the central fiber in Figure 3D), owing to the restraint exerted by the rigid structure (the width of the fibers is approximately reduced from 17 to 13 μm). Thus, in spite of the intense softening of the more internal parts of the thickness of the cell walls during pyrolysis, the presence of the phenolic resin (and possibly the thermosetting adhesive) gives some rigidity to the more external layer, which appears to be sufficient to avoid collapse of the honeycomb structure. Indeed, phenolic resins are often used as matrixes to protect and reinforce the fibers contained within the composite structure.

3.2. Thermogravimetric Behavior. As anticipated, weight loss curves of the composite material are measured for heating rates between 3 and 7 K/min up to a final temperature of 950 K. Figure 4 reports an example of the solid mass fraction and the corresponding first and second time derivatives versus time for a heating rate of 5 K/min. The second derivative of the solid mass fraction is extensively used in the analysis of thermogravimetric data to define some characteristic points of the weight loss rate curves, specifically the initial and peak temperatures of the shoulder zones (see, for instance, refs 35 and 36). The beginning of the shoulder zone is associated with a characteristic temperature defined by extrapolating the slope of the

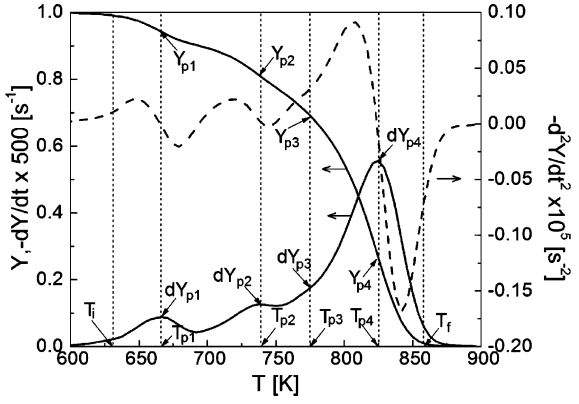

Figure 4. Mass fraction, Y, and the first and second time derivatives, $-dY/dt$ and $-d^2Y/dt^2$, for the composite material in air versus time for a heating rate of 5 K/min up to 950 K with the definition of thermogravimetric parameters: initial degradation temperature, T_i, characteristic temperatures, T_{pi} (temperatures corresponding to the shoulders and peaks of the mass release rate curve), and corresponding mass fractions, Y_{pi}, and rates of mass loss, dY_{pi}, and the final degradation temperature, T_f.

devolatilization rate in correspondence with the first local maximum in $-d^2Y/dt^2$ (up to the zero level of the Y axis). Then, the decomposition temperature of this zone is defined by the point where $-d^2Y/dt^2$ attains the value nearest to zero in this region. Indeed, apart from providing the main features of the weight loss process, the curves can also be used to introduce the following parameters: initial degradation temperature, T_i (the temperature corresponding to the release of 1% of the total

dx.doi.org/10.1021/ie402470z | Ind. Eng. Chem. Res. 2013, 52, 14574−14582

volatiles), characteristic temperatures, T_{pi} (temperatures corresponding to the shoulders and peaks of the mass release rate curve), and corresponding mass fractions, Y_{pi}, and rates of mass loss, dY_{pi}, and the final degradation temperature, T_f (the temperature corresponding to the release of 99% of the volatile products). As expected, the values of these parameters are somewhat affected by the heating rate, as indicated in Table 1. In general, as observed in previous thermogravimetric studies,[37,38] the onset of the various reaction stages is displaced at successively higher temperatures, and the corresponding peak rates tend to increase as the heating rate is increased. For the composite material under study, the oxidation process approximately begins for temperatures above 600 K (T_i between 622 and 635 K) and is practically terminated for temperatures above 900 K (T_f between 836 and 860 K). The examination of the curves reported in Figure 4 underlines the presence of two consecutive peaks, a shoulder and a further peak. The highest peak is attained at high temperatures (814−834 K, for the range of heating rates investigated), whereas the other characteristic points are positioned, in the order, at temperatures between 661 and 673 K, 720 and 746 K, and 778 and 800 K. Solid oxidation generally occurs according to two main stages representing oxidative degradation (volatilization) of the original material and combustion of the char produced.[28] Using the information gained from the pyrolysis experiments that the yields of solid residue are around 56%, it could be reasonably estimated that a temperature of around 800 K demarks the volatilization and combustion zones. However, the char yields depend on the pyrolysis conditions; in particular, they decrease as the reaction temperature increases.[39] Hence, in the presence of oxygen, it is likely that the combustion process begins at lower temperatures, when the amount of the charred solid residue is higher than the value obtained in an inert environment (at higher temperatures). Anyway, it is evident that solid decomposition takes place according to three main steps, characterized by the release of relatively small amounts of volatiles, followed by a final reaction describing combustion of the char, which gives rise to the peak rate and the production of the largest amount of volatiles.

Table 1. Characteristic Parameters of the Thermogravimetric Curves Measured in Air at Three Heating Rates, h, of the Composite Material versus the Heating Rate: Initial Degradation Temperature, T_i, Temperatures, T_{pi}, at the Shoulders and Peaks of the Mass Release Rate Curve and Corresponding Mass Fractions, Y_{pi}, and Rates of Mass Loss, dY_{pi}, and the Final Degradation Temperature, T_f

	h [K/min]		
parameter	3	5	7
T_i [K]	622	630	635
T_{p1} [K]	661	665	673
Y_{p1}	0.91	0.94	0.95
$-(dY/dt)_{p1} \times 10^3$ [s^{-1}]	0.16	0.18	0.21
T_{p2} [K]	720	738	746
Y_{p2}	0.78	0.81	0.82
$-(dY/dt)_{p2} \times 10^3$ [s^{-1}]	0.14	0.26	0.32
T_{p3} [K]	778	790	800
Y_{p3}	0.54	0.61	0.62
$-(dY/dt)_{p3} \times 10^3$ [s^{-1}]	0.33	0.35	0.86
T_{p4} [K]	814	825	834
Y_{p4}	0.21	0.27	0.24
$-(dY/dt)_{p4} \times 10^3$ [s^{-1}]	0.65	1.14	1.90
T_f [K]	836	858	860

As stated in the Introduction, the combustion behavior of this commercial composite material has never been studied, although thermal decomposition of polyaramid fibers has been given consideration in a number of studies.[8−11] These studies report that pyrolysis begins with the rupture of hydrogen bonds (590 K), accompanied by a small steam release, followed by a two-step weight loss (673−760 and 760−880 K) attributable to the homolytic and heterolytic rupture of the aramid unit, respectively. Finally, at higher temperatures, condensation reactions may further occur, leading to char. It is interesting to observe that weight loss for the composite material under study starts at about the same temperature as that for the polyaramid fibers, whereas in accordance with the related temperature ranges, the first two peaks, on the one side, and the shoulder close to the oxidation peak, on the other side, can be reasonably associated with the two decomposition paths indicated above. However, the presence of oxygen, which already plays a role at low temperatures by enhancing decomposition,[38] drastically modifies the weight loss dynamics at high temperatures with the onset of heterogeneous combustion reactions. Moreover, it should also be taken into account that the phenolic resin, in the form of a surface coating, in the first place contributes with its own degradation characteristics. Thermogravimetric curves show that the main decomposition reaction typically occurs over a temperature range of 673−773 K, yielding a large amount of char residue (about 60−70% of the original mass).[34] In the second and more important place, it may also modify the thermal and chemical resistance of the underneath material.

An interesting result in this regard is obtained by studying the oxidation of char, previously produced from the pyrolysis experiments at 950 K. It is worth recalling that weight loss measurements for the composite material are made using thin strips with both sides coated with phenolic resin, whereas char is oxidized in the form of a thin powdered layer. From the comparison between the two samples shown in Figure 5 (heating rate 5 K/min), it appears that the weight loss begins approximately at the same temperature (possibly owing to the still significant volatile content of the char), but the oxidation peak temperature of the char precedes that for the composite. More precisely, the peak rate is 80 K less (peak position at 747 K versus 825 K of the composite material). This behavior can be attributed, in the first place, to the shielding effect exerted by the

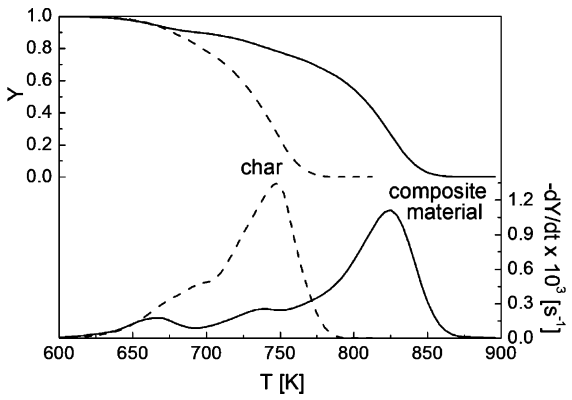

Figure 5. Mass fraction, Y, and mass loss rate, $-dY/dt$, for the composite material and char (produced from pyrolysis of a thick sample at 950 K) in air versus time for a heating rate of 5 K/min up to 950 K.

dx.doi.org/10.1021/ie402470z | Ind. Eng. Chem. Res. 2013, 52, 14574−14582

phenolic coating with respect to the fiber sheet. Indeed, the highly aromatic char produced from degradation of the resin is scarcely reactive at low temperatures, so that, as long as its structure is preserved, oxygen diffusion to the underneath more reactive char is hindered. This feature is lost for the granular char, where the more reactive char produced from degradation of the aramid fiber sheet becomes directly accessible to oxygen (the percentage of the phenolic char is small anyway). Moreover, in this case, the surface area is certainly higher, thus representing another factor that increases the reactivity.

3.3. Oxidation Kinetics. Analysis of the thermogravimetric curves indicates that the composite honeycomb material in air presents two main reaction stages, corresponding to oxidative decomposition (of the material) and combustion of the resulting char. Again, in accordance with the qualitative features shown by the various curves, the two stages require at least three reactions (most likely corresponding to volatiles released from the rupture of hydrogen bonds and homolytic and heterolytic rupture of the aramid unit) and one reaction (volatiles released from char combustion), respectively. As is generally assumed in the formulation of multistep reaction mechanisms for the oxidation of organic and synthetic polymers,[24,27,28,31,40,41] four parallel reactions are proposed here:

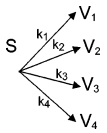

(a1)
(a2)
(a3)
(a4)

where S is the composite material that produces the lumped volatile products V_i (i = 1, 4). From the chemical point of view, reactions (a1)−(a3) are associated with solid fuel volatilization and reaction (a4) with char oxidation. In practice, solid volatilization and char combustion are sequential processes, but the parallel reaction mechanism is more flexible because it can easily guarantee this feature by an appropriate set of parameter values and, at the same time, can describe well the possible overlap between reactions pertinent to either the volatilization or combustion stage. The reaction rates present the usual Arrhenius dependence (A_i are the preexponential factors and E_i the activation energies) on the temperature and a power law dependence, exponent n_i, on the solid mass fraction. The latter treatment takes into account evolution of the pore surface area during conversion.[42] In fact, the heterogeneous combustion rate can always be expressed by means of a chemical kinetic term, generally accounting for temperature and reactant partial pressure effects, and a structural term, implicitly or explicitly assumed to describe the effects of the available internal surface or active sites, and pore evolution, which is usually related to the solid mass fraction. Because the sample temperature, T, is a known function of time, the mathematical model consists of four ordinary differential equations for the mass fractions, Y_i, of the reacting solid fuel:

$$\frac{dY_i}{dt} = A_i \exp\left(-\frac{E_i}{RT}\right) Y_i^{n_i}; \qquad Y_i(0) = \nu_i, \qquad i = 1,\ 4 \tag{1a-4a;1b-4b}$$

In addition to the kinetic parameters (A_i, E_i, and n_i), the mass fractions of the lumped classes of volatiles generated, ν_i, usually indicated as stoichiometric coefficients, should also be estimated.

The parameters are estimated through the numerical solution (implicit Euler method) of the mass conservation equations and the application of a direct method for minimization of the objective function, which considers simultaneously both integral (TG) and differential (DTG) data for the various heating rates, following the method already described[23] and the references cited therein. It is a direct method, belonging to the class of comparison methods, that is used to find the minimum of a scalar function of n independent variables. In contrast to gradient methods, direct methods do not require the derivatives of the scalar function. Different criteria can be used for selecting the orientation of the axis along which the optimum of F should be found. The approach used here combines the Rosenbrock formulas and the golden section method. The objective function, for a first-basis estimate, can be expressed in differential form as

$$F = \sum_{i=1,M} \sum_{i=1,N} \left[\frac{(dY_{ij})_{exp} - (dY_{ij})_{sim}}{(dY_{ij})_{exp} + (dY_{ij})_{sim}} \right]^2 \tag{5}$$

where i represents the experimental (exp) or simulated (sim) time derivative (dY) of the solid fraction at time t, j is the heating rate (N is the number of experimental points and M the number of experiments carried out by varying the heating rate), and the scale parameter, f_j, is expressed as

$$f_j = \frac{1}{\max_j[(dY_{ij})_{exp}]^2} \tag{6}$$

The kinetic parameter values determined in this way are then used as a set of initial values for the final estimates based on the objective function expressed in integral form

$$F = \sum_{i=1,M} \sum_{i=1,N} \left[\frac{(Y_{ij})_{exp} - (Y_{ij})_{sim}}{(Y_{ij})_{exp} + (Y_{ij})_{sim}} \right]^2 \tag{7}$$

The application of the parameter estimation procedure to multiple curves also allows the compensation effect to be avoided, that is, the possibility of different preexponential factor and activation energy combinations to describe reasonably well the same weight-loss curve. Indeed, only one set of data can predict the behavior of the material at several heating rates, consisting of the displacement of the weight-loss curves toward successively shorter times for successively more severe thermal conditions. Also, there is always the possibility that only a local minimum is found, instead of the absolute minimum. However, several combinations of kinetic parameters have been tested, and those chosen are always associated with the lowest value of the objective function, F. The minimization procedure based on the differential form of F presents the interesting feature of capturing all of the details of the experiments. However, because small experimental errors in the computation of the derivative can result in incorrect kinetic data, the integral form is also used for further improvement in the kinetic constants.

The estimation procedure is implemented by requiring the same parameter values for all of the measured curves, with the exception of the stoichiometric coefficients, which are allowed to show small variations as a consequence of the dependence of the amounts of volatiles released during the first reaction stage on the heating rate. Finally, deviations between measurements and model predictions, dev_{TG} and dev_{DTG}, are defined as in a previous study.[23]

The estimated values of the kinetic parameters and deviations between predictions and measurements are listed in Table 2. Figure 6 shows an example of the predicted dynamics of the single components and a comparison between measurements and predictions (heating rate of 5 K/min), whereas a comparison for the integral and differential data for all of the heating

dx.doi.org/10.1021/ie402470z | Ind. Eng. Chem. Res. 2013, 52, 14574−14582

Table 2. Estimated Kinetic Parameters (Activation Energy E, Preexponential Factor A, Reaction Order n, and Stoichiometric Coefficient ν) for Combustion of the Composite Material and Corresponding Deviations between the Measured and Simulated Integral (dev_{TG}) and Differential (dev_{DTG}) Curves (the Parameters Are Invariant with the Heating Rate, h, Except for Small Variations on the Stoichiometric Coefficients)

	h [K/min]		
parameter	3	5	7
E_1 [kJ/mol]		198.4	
A_1 [s^{-1}]		1.21×10^{13}	
n_1		0.90	
ν_1	0.11	0.09	0.08
E_2 [kJ/mol]		190.1	
A_2 [s^{-1}]		1.02×10^{11}	
n_2		0.85	
ν_2	0.11	0.11	0.11
E_3 [kJ/mol]		212.9	
A_3 [s^{-1}]		5.61×10^{11}	
n_3		0.80	
ν_3	0.12	0.11	0.10
E_4 [kJ/mol]		256.3	
A_4 [s^{-1}]		5.88×10^{13}	
n_4		0.80	
ν_4	0.66	0.69	0.71
% dev_{TG}	1.07	0.85	0.77
% dev_{DTG}	1.83	1.96	1.10

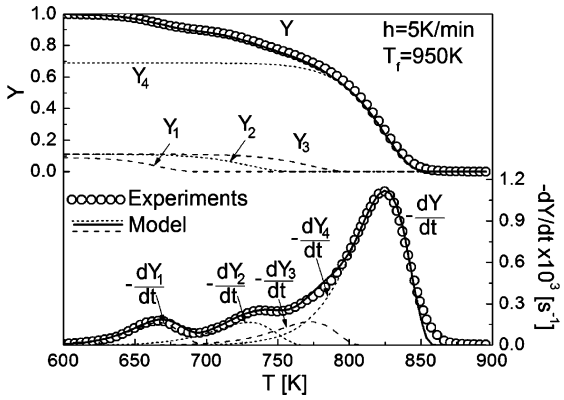

Figure 6. Comparison between the measured (symbols) and simulated (solid lines) mass fractions and the rate of mass loss for the composite material in air with a heating rate, h, of 5 K/min up to 950 K. Thin lines with various styles denote the predicted evolution of the mass fraction and rate of mass loss for the various reaction zones: 1, 2, and 3, volatilization of the composite material; 4, combustion of the char (kinetic parameters are listed in Table 2).

conditions is shown in Figure 7. The kinetic mechanism (a1−a4) and the related parameters provide accurate predictions of the measured integral and differential curves in all cases. Moreover, it can be seen that variations in the stoichiometric coefficients are small, and average values can be used in practical applications. The three reactions for the volatilization stage present rather high values of the activation energy (198, 190, and 213 kJ/mol) with amounts of released volatile products around 9, 11, and 11%, respectively. As expected, some overlap exists between the reaction zones, especially for the two located at higher temperatures. Although the decomposition reactions of aramid

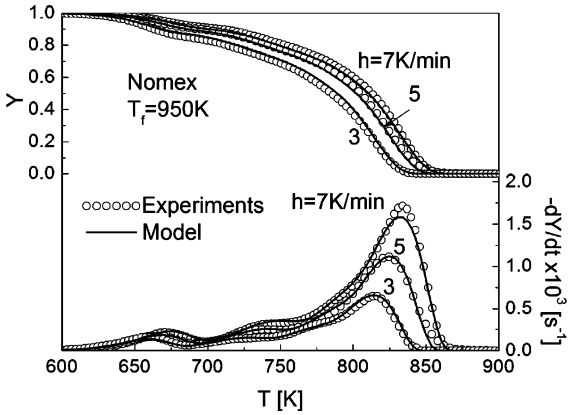

Figure 7. Comparison between the measured (symbols) and simulated (solid lines) thermogravimetric curves for the composite material at various heating rates, h, in air up to a temperature of 950 K (kinetic parameters are listed in Table 2).

fibers have been studied,[8−11] no estimates of the corresponding kinetic constants are available. So, a comparison cannot be made. For the oxidation reaction, an activation energy of 256 kJ/mol is estimated, which is close to the upper limit of the range typically reported for carbonaceous materials produced from the degradation of both organic[42] and synthetic[27,31] polymers, testifying high reactivity only at high temperatures. It is worth noticing that, in all cases, the reaction order remains very close to 1 (values in the range 0.8−0.9). Finally, for comparison purposes, the thermogravimetric curve measured for the powdered char sample is subjected to kinetic analysis using a two-step mechanism in accordance with previous findings.[25] The actual oxidation step, accounting for the release of about 80% of the volatile matter, is well described by an activation energy of 190 kJ/mol (preexponential factor 1.7×10^{12} s^{-1}; reaction order 0.9) (not shown). This is significantly lower than the value estimated for the char oxidation step of the complete mechanism and practically coincident with the results obtained for lignocellulosic chars.[42] This finding further confirms the important role played by the surface coating of the phenolic char in the scarce oxidation reactivity of the composite material.

The composition of the gaseous products generated during volatilization of the honeycomb composite material and combustion of the char is not measured. It can be reasonably assumed that the contribution to the gas phase due to the phenolic resin is small because of its very low percentage in the composite material and the high yields of char produced upon pyrolysis. Moreover, the composition of the volatile product during the various stages of the degradation process of polyaramid fibers is already available.[12] Gases include HCN, NO_2, CO, CO_2, and H_2O, with amounts that depend on the reaction temperature or, in other words, with production rates directly related to the rate of weight loss of the solid phase. Therefore, it can be expected that, at least for the volatilization stage of the composite material under study, a similar composition is established. In the modeling of practical systems, gas-phase combustion can be described by coupling the equations for the transport phenomena incorporating the heterogeneous kinetics, as determined in this study, and adequate reaction mechanisms for the various gas-phase species.

dx.doi.org/10.1021/ie402470z | Ind. Eng. Chem. Res. 2013, 52, 14574−14582

4. CONCLUSIONS

The thermogravimetric behavior has been investigated and a kinetic mechanism has been, for the first time, proposed for the heterogeneous combustion of a honeycomb composite consisting of aramid fiber sheets dipped in a phenolic resin, largely used as the core in sandwich panels.

The honeycomb structure survives after pyrolytic degradation at high temperature, although accompanied by significant anisotropic shrinkage. Examination of the char morphology shows that the thickness of the cell walls is approximately doubled but the internal void space of the cell is more than halved. More in detail, it is evident that the more internal part of the cell thickness, consisting of an aramid fiber sheet, softens and, following generation of the volatile products, swells, giving rise, upon further heating, to a charred highly porous structure. However, the more external part of the aramid material, trapped by the rigid charred residue generated from decomposition of the phenolic resin, partly preserves the original shape of the fibers. This rigid and low-porosity external char layer prevents collapse of the honeycomb structure.

Thermogravimetric measurements in air suggest a multistep process corresponding to oxidative decomposition of the composite material and combustion of the resulting char. Oxidative decomposition, approximately occurring for temperatures between 600 and 800 K, is well described by three reactions, with a certain degree of overlap, causing the release of about 9, 11, and 11% of the initial sample mass (activation energies of 198, 190, and 213 kJ/mol). Char combustion mainly occurs at temperatures above 800 K and is described by a one-step reaction with an activation energy of 256 kJ/mol. The reduced char reactivity can be attributed to the properties of char generated from the phenolic resin, which acts as a shield for the underneath char generated from the aramid fiber sheet, hindering oxygen diffusion.

AUTHOR INFORMATION

Corresponding Author

*Tel: 39-081-7682232. Fax: 39-081-5936936. E-mail: branca@irc.cnr.it.

Notes

The authors declare no competing financial interest.

ACKNOWLEDGMENTS

This work is part of the activities carried out in the framework of the project COCET "Comportamento di Materiali Compositi in Condizioni Estreme: Alta Temperatura" (PON02_00029_3206086/F1), coordinated by IMAST and funded by the Italian Ministry of Instruction, University and Research (MIUR), the partial support of which is gratefully acknowledged. The authors also thank Luciano Cortese (Istituto di Ricerche sulla Combustione, CNR, Napoli, Italy) for the SEM images of the samples.

REFERENCES

(1) Mouritz, A. P.; Gibson, A. G. *Fire Properties of Polymer Composite Material*; Springer: Dordrecht, The Netherlands, 2006.

(2) Mouritz, A. P.; Gardiner, C. P. Compression properties of fire-damaged polymer sandwich composites. *Composites, Part A* **2002**, *33*, 609.

(3) Goodrich, T. W.; Lattimer, B. Y. Fire decomposition effects on sandwich composite materials. *Composites, Part A* **2012**, *43*, 803.

(4) Heimbs, S.; Schmeer, S.; Middendorf, P.; Maier, M. Strain rate effects in phenolic composites and phenolic-impregnated honeycomb structures. *Compos. Sci. Technol.* **2007**, *67*, 2827.

(5) Yang, C. Q.; He, Q.; Lyon, R. E.; Hu, Y. Investigation of the flammability of different textile fabrics using micro-scale combustion calorimetry. *Polym. Degrad. Stab.* **2010**, *95*, 108.

(6) Horrocks, A. R.; Nazare, S.; Masood, R.; Kandola, B.; Price, D. Surface modification of fabrics for improved flash-fire resistance using atmospheric pressure plasma in the presence of a functionalized clay and polysiloxane. *Polym. Adv. Technol.* **2011**, *22*, 22.

(7) Osorio, A. F.; Fernandez-Pello, C.; Urban, D. L.; Ruff, G. A. Limiting conditions for flame spread in fire resistant fabrics. *Proc. Combust. Inst.* **2013**, *34*, 2691.

(8) Villar-Rodil, S.; Martinez-Alonso, A.; Tascon, J. M. D. Studies on pyrolysis of Nomex polyaramid fibers. *J. Anal. Appl. Pyrolysis* **2001**, *58*−*59*, 105.

(9) Villar-Rodil, S.; Paredes, J. I.; Martinez-Alonso, A.; Tascon, J. M. D. Atomic Force Microscopy and Infrared Spectroscopy Studies of the Thermal Degradation of Nomex Aramid Fibers. *Chem. Mater.* **2001**, *13*, 4297.

(10) Suarez-Garcia, F.; Villar-Rodil, S.; Blanco, C. G.; Martinez-Alonso, A.; Tascon, J. M. D. Effect of Phosphoric Acid on Chemical Transformations during Nomex Pyrolysis. *Chem. Mater.* **2004**, *16*, 2639.

(11) Villar-Rodil, S.; Suarez-Garcia, F.; Paredes, J. I.; Martinez-Alonso, A.; Tascon, J. M. D. Activated Carbon Materials of Uniform Porosity from Polyaramid Fibers. *Chem. Mater.* **2005**, *17*, 5893.

(12) Cai, G. M.; Yu, W. D. Study on the thermal degradation of high performance fibers by TG/FTIR and Py-GC/MS. *J. Therm. Anal. Calorim.* **2011**, *104*, 757.

(13) Nyden, M. R.; Brown, J. E.; Lomakin, S. M. Flammability properties of honeycomb composites and phenol−formaldehyde resins. *Fire and polymers II: materials and tests for hazard prevention*; ACS Symposium Series 599; American Chemical Society: Washington, DC, 1994; p 245−255.

(14) Mouritz, A. P.; Feih, S.; Kandare, E.; Mathys, Z.; Gibson, A. G.; Des Jardin, P E.; Case, S. W.; Lattimer, B. Y. Review of fire structural modelling of polymer composites. *Composites, Part A* **2009**, *40*, 1800.

(15) Di Blasi, C.; Branca, C. A mathematical model for the non-steady decomposition of intumescent coatings. *AIChE J.* **2001**, *47*, 2359.

(16) Staggs, J. E. J.; Crewe, R. J.; Butler, R. A theoretical and experimental investigation of intumescent behavior in protective coatings for structural steel. *Chem. Eng. Sci.* **2012**, *71*, 239.

(17) Kandare, E.; Griffin, G. J.; Feih, S.; Gibson, A. G.; Lattimer, B. Y.; Mouritz, A. P. Fire structural modeling of fibre−polymer laminates protected with an intumescent coating. *Composites, Part A* **2012**, *43*, 793.

(18) Di Blasi, C.; Galgano, A.; Branca, C. Modeling the thermal degradation of poly(methyl methacrylate)/carbon nanotube nanocomposites. *Polym. Degrad. Stab.* **2013**, *98*, 266.

(19) Galgano, A.; Di Blasi, C.; Branca, C.; Milella, E. Thermal response to fire of a fibre reinforced sandwich panel: model formulation, selection of intrinsic properties and experimental validation. *Polym. Degrad. Stab.* **2009**, *94*, 1267.

(20) Galgano, A.; Di Blasi, C.; Milella, E. Sensitivity analysis of a predictive model for the fire behavior of a sandwich panel. *Polym. Degrad. Stab.* **2010**, *95*, 2430.

(21) http://www.hexcel.com/Resources/DataSheets/Honeycomb-Data-Sheets/HRH_10_eu.pdf.

(22) Lanzetta, M.; Di Blasi, C.; Buonanno, F. An experimental investigation of heat transfer limitations in the flash pyrolysis of cellulose. *Ind. Eng. Chem. Res.* **1997**, *36*, 542.

(23) Branca, C.; Di Blasi, C.; Horacek, H. Analysis of the combustion kinetics and the thermal behaviour of an intumescent system. *Ind. Eng. Chem. Res.* **2002**, *41*, 2104.

(24) Branca, C.; Di Blasi, C.; Casu, A.; Morone, V.; Costa, C. Reaction kinetics and morphological changes of a rigid polyurethane foam during combustion. *Thermochim. Acta* **2003**, *399*, 127.

(25) Branca, C.; Di Blasi, C. Devolatilization and combustion kinetics of wood chars. *Energy Fuels* **2003**, *17*, 1609.

(26) Branca, C.; Di Blasi, C.; Elefante, R. Devolatilization and heterogeneous combustion of wood fast pyrolysis oils. *Ind. Eng. Chem. Res.* **2005**, *44*, 799.
(27) Branca, C.; Di Blasi, C.; Galgano, A.; Milella, E. Thermal and kinetic characterization of a toughened epoxy resin reinforced with carbon fibres. *Thermochim. Acta* **2011**, *517*, 53.
(28) Branca, C.; Di Blasi, C. A unified mechanism of the combustion reactions of lignocellulosic fuels. *Thermochim. Acta* **2013**, *565*, 58.
(29) Branca, C.; Di Blasi, C. Global intrinsic kinetics of wood oxidation. *Fuel* **2004**, *83*, 81.
(30) Varhegyi, G.; Meszaros, E.; Antal, M. J.; Bourke, J.; Jakab, E. Combustion kinetics of corncob charcoal and partially demineralized corncob charcoal in the kinetic regime. *Ind. Eng. Chem. Res.* **2006**, *45*, 4962.
(31) Di Blasi, C.; Branca, C.; Galgano, A.; Moricone, R.; Milella, E. Oxidation of a carbon/glass reinforced cyanate ester composite. *Polym. Degrad. Stab.* **2009**, *94*, 1962.
(32) Di Blasi, C.; Branca, C.; Galgano, A. Biomass screening for the production of furfural via thermal decomposition. *Ind. Eng. Chem. Res.* **2010**, *49*, 2658.
(33) Di Blasi, C. Influences of model assumptions on the predictions of cellulose pyrolysis in the heat transfer controlled regime. *Fuel* **1996**, *75*, 58.
(34) Mouritz, A. P.; Mathys, Z.; Gibson, A. G. Heat release of polymer composites in fire. *Composites, Part A* **2006**, *37*, 1040.
(35) Gronli, M. G.; Várhegyi, G.; Di Blasi, C. Thermogravimetric analysis and devolatilization kinetics of wood. *Ind. Eng. Chem. Res.* **2002**, *41*, 4201.
(36) Várhegyi, G.; Gronli, M. G.; Di Blasi, C. Effects of sample origin, extraction and hot water washing on the devolatilization kinetics of chestnut wood. *Ind. Eng. Chem. Res.* **2004**, *43*, 2356.
(37) Branca, C.; Albano, A.; Di Blasi, C. Critical evaluation of wood devolatilization mechanisms. *Thermochim. Acta* **2005**, *429*, 133.
(38) Brostrom, M.; Nordin, A.; Pommer, L.; Branca, C.; Di Blasi, C. Influence of torrefaction on the devolatilization and oxidation kinetics of wood. *J. Anal. Appl. Pyrolysis* **2012**, *96*, 100.
(39) Di Blasi, C.; Branca, C.; Santoro, A.; Perez Bermudez, R. A. Weight loss dynamics of wood chips under fast radiative heating. *J. Anal. Appl. Pyrolysis* **2001**, *57*, 77.
(40) Várhegyi, G.; Czégény, Z.; Liu, C.; McAdam, K. Thermogravimetric analysis of tobacco combustion assuming DAEM devolatilization and empirical char-burnoff kinetics. *Ind. Eng. Chem. Res.* **2011**, *49*, 1591.
(41) Várhegyi, G.; Sebestyen, Z.; Czegeny, Z.; Lezsovits, F.; Konczol, S. Combustion kinetics of biomass material in the kinetic regime. *Energy Fuels* **2012**, *26*, 1323.
(42) Di Blasi, C. Combustion and gasification rates of lignocellulosic chars. *Prog. Energ. Combust. Sci.* **2009**, *35*, 121.